Advanced and Sustainable Technologies (ASET) eISSN 2976-2294
Volume 1, No 2, December 2022 [20-29]

Multi-Objective Optimization of Absorber Piston Rod Design Parameter using Response Surface Methodology

Muhammad Zaki Zamri[1*]

[1]Faculty of Mechanical Engineering & Technology, Universiti Malaysia Perlis, Perlis, Malaysia.

Received 19 July 2022, Revised 1 Sept 2022, Accepted 18 Sept 2022

ABSTRACT

Car absorbers provide a comfortable ride and improve ride handling by delivering road wheel contact. The typical car absorber problems are oil leakage and piston rod wear-out due to the lateral friction between the shell case and piston rod. The piston rod can bend and rupture when exposed to higher vibration exerting high impact force. This study focuses on optimizing car absorber piston rod design parameters via finite element analysis. The response surface methodology (RSM) was utilized to create the design of the numerical experiment. The piston rod parameters (i.e., length of the piston rod, the piston rod diameter #1, and the piston rod diameter #2) were optimized to reduce the stress and displacement of the piston rod. The optimization results revealed that the optimum parameters were 254 mm in piston length, 24.79 mm in diameter #1, and 15 mm in diameter #2. With the optimized piston rod parameters, the stress and displacement of the piston were 1.65048E+007 and 0.007569 mm, respectively. The most significant factors that influence the responses were also studied. The suggested optimized factors and responses were validated in the finite element simulation.

Keywords: Response surface methodology, Finite element analysis, Optimization, Piston rod

1. INTRODUCTION

Ride comfort and road control are vital factors in assessing suspension performance [1]. Ride comfort corresponds to the total increasing speed of the vehicle body. At the same time, street dealing relates to the relocation between the vehicle body and the tires. Most vehicle suspension system consists of a damper, a spring, and an arrangement of linkages [2]. Each of these components has its functional reason inside the suspension system. The spring component gives vitality storage by giving stiffness [3], the damping component gives vitality scattering as an element of its damping coefficient, and the linkages give instrument imperatives on the suspension movement and control movement [4]. There are three types of suspension: passive suspension, fully active suspension, and semi-active suspension [5]. An absorber is a standout amongst the most critical segments in the automotive suspension system, which can reduce vibration and increase comfort and car compliance by changing the kinetic energy of vibration between the wheel and body into heat energy by specific orifices. The inside of a shock absorber consists of the critical part, in which the piston rod ensures that a shock absorber works appropriately [6].

With an increment in car driving velocity, the absorbers have numerous practical issues caused by the lateral friction between the seal and piston rod [7], which could lead to functionality loss in the beginning stage. For example, oil leakage and piston rods wear out because of changing the kinetic energy of vibration between the car body and wheel into heat energy at specific orifices [8]. Since the piston rod surface is subjected to dynamic friction [9] and exposure to serious wear-out in the car's lateral movement, the absorber leaks damping oil. Moreover, when the velocity of

*Corresponding author: zakizamri07@gmail.com

a car increase, that absorber will be exposed to a higher vibration that can exert a high impact force toward the piston rod [10]. This can make the structure of the piston rod become bend and rupture. For an overall evaluation of dynamic forces and the lateral friction conditions, many of the absorbers had been replaced due to surface damage from road tests [11]. Strains and accelerations of the piston rod in both the axle plane and the wheel are tested by many bench tests of brand-new absorbers. Because of the piston rod's surface damage, a higher economic loss has to be faced by both the car users and the maker. Hence, making a suitable design parameter for a piston rod is essential. Therefore, optimizing the absorber piston is crucial to ensure the maximum durability and reliability of the car absorber. The optimization could be achieved using various optimization methods such as response surface methodology [12], full factorial [13], and Taguchi [14].

Response surface methodology (RSM) gathers statistical and mathematical techniques for exact model building [15]. With the wisely designed experiments, the target is to optimize the response (output variables) affected by a few independent variables (input variables). The experiment is a sequence of tests called runs where changes are done in the input variables to recognize the cause for changes in the output response. Initially, RSM was produced for experimental model responses [16] and migrated into various experiments. The distinction is in the sort of error created by the response. In physical analyses, the mistake can be expected. In RSM, the error is assumed to be random. The use of RSM to design optimization is targeted at diminishing the cost of expensive analysis techniques such as CFD analysis [17] or finite element method [18] and their related numerical simulation. The issue can be approximated with smooth capacities that enhance the joining of the optimization procedure since they reduce the result of noise and consider the utilization of derivative-based algorithms [19].

In the current study, optimization was carried out for the car absorber piston rod using response surface methodology. Three design parameters of the piston rod were considered in the optimization process. Two responses, i.e., stress and displacement of the piston rod, were studied in finite element analysis. Besides, the most significant factor was also identified in the current optimization study. The optimization recommended the optimized value of each parameter, and the validation was confirmed with the finite element software.

2. MATERIAL AND METHODS

The damper is usually known as an absorber. An absorber system involves many components: cylinder, shell case, piston rod, piston valve, oil chamber, and base valve. Most part absorbers are cylinders working in shell cases loaded with fluid. However, this study only focuses on the piston rod. Figure 1(a) shows the absorber system's selected part (piston rod) used in the current study. The front view of the piston rod model with labels is depicted in Figure 1(b). The piston rod with label A is the length of the piston rod, B is diameter #1, and C is diameter #2. The shape of the piston rod is a cylinder shape, and the parameters of the piston rod (A, B, and C) are combined based on the central composite design (CCD). The range of length is from 254 mm to 314 mm. The range of diameter #1 is from 15 mm to 24.8 mm, and the range of diameter #2 is from 10 mm to 15 mm. The diameter of the upper part (Diameter #1) is larger than the diameter of the lower part (Diameter #2), as clearly shown in Figure 1(b).

Using the combination of parameters by CCD, the piston rod's 3-dimensional (3D) model was created using Solidworks. The piston rod material was defined as Alloy Steel, and the material properties are summarized in Table 1. The fixed boundary condition was defined at the bottom of the piston model. The exerted downward force (2479.48 N) was applied on the top of the piston rod, which is assumed to be the load from the vehicle. After that, the 3D model was used for the finite element analysis. Analysis of variance (ANOVA) statistically processed the simulation results in determining the regression and significance of the quadratic model.

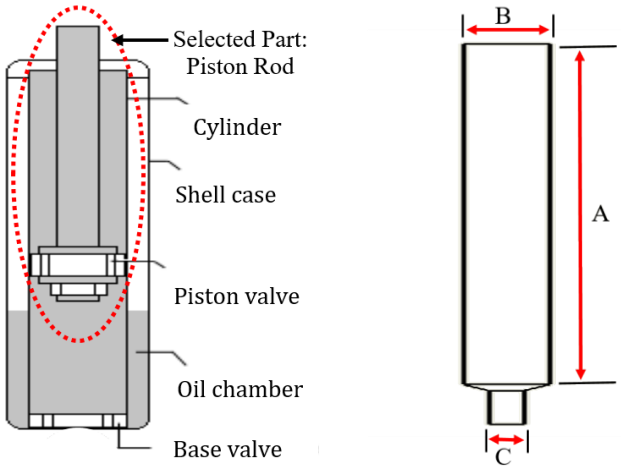

Figure 1: (a) Piston rod of the absorber and (b) piston rod model in simulation.

Table 1: Material properties of alloy steel.

Property	Value	Units
Elastic Modulus	2.1e+011	N/m^2
Poisson's Ratio	0.28	N/A
Shear Modulus	7.9e010	N/m^2
Density	7700	Kg/m^3
Tensile Strength	723825600	N/m^2
Yield Strength	620422000	N/m^2

The design parameters selected are the length of the piston rod, diameter #1 of the upper part, and diameter #2 of the lower part of the piston rod. The responses chosen are maximum stress and maximum displacement. This work aims to reduce the maximum stress and maximum displacement through the factors when the force or load is exerted toward the piston. Therefore, factors and responses are interrelated, affecting each other in order to achieve the goals. According to the normal stress ($\sigma = F_n / A$) formula, stress is inversely proportional to area. In a larger area, the stress will be lower. This concept is applicable to reduce the maximum stress of the piston rod. However, the area cannot be too large because the piston rod needs to be inserted into the shell case. For the maximum displacement, the piston rod size cannot be too small because the heat produced by oscillating the piston rod will distribute to the entire body more quickly. This situation can make the piston rod easier to expend, which can encourage the displacement of the piston rod to occur.

A main feature of RSM is the design of experiments commonly known as DoE. With the cautious design of experiments, the purpose is to optimize the response (output variable) affected by various independent variables (input variables). The experiments are a sequence of tests known as runs where changes are done in the input variable to recognize the cause to alter the output response. The central composite design (CCD) [20] was chosen for the experiment design in RSM. CCD can be presented as a choice to full factorial design that contains three varying levels (low level "-1", medium "0" and high level "+1") of all combinations of factors such as length of the piston rod, diameter #1 of the piston rod and diameter #2 of the piston rod as shown in Table 2. The expected number of the numerical experiment is 20 runs for different combinations of different factor levels. The equation of CCD is 2^k+2k+6. K represents the number of factors, 2^k is for factorial points, 2k is for axial points, and 6 is a center point. The center point depends on the number of factors (such as two factors use five center points and three factors use six center points).

Table 2: Factor and levels -1, 0, and +1 used in the CCD.

No	Factor	Unit	Level		
			Low (-1)	Medium (0)	High (-1)
1	Length of the piston rod	mm	254	284	314
2	Diameter #1	mm	15	19.9	24.8
3	Diameter #2	mm	10	12.5	15

3. RESULTS AND DISCUSSION

This optimization study aims to minimize the maximum stress (Y_1) and maximum displacement (Y_2) of a suspension piston rod to ensure a more reliable and durable system. Stress and displacement reduction can prevent the rod piston from failing and rupturing, affecting the suspension performance. Table 3 summarizes the results of the twenty runs that were conducted in this study. The highest maximum stress (Y_1 = 3.55736E+007 Pa) was observed in run 4 when the medium length, medium diameter #1, and smallest diameter #2 were used. While the lowest maximum stress (Y_1 = 1.47291E+007 Pa) was observed in run 19 with the shortest length, smallest diameter #1, and highest diameter #2. Minimum stress and displacement are suitable for a piston rod as they reduce failure and rupture. However, a higher maximum displacement (Y_2 = 0.01978 mm) was observed in run 1 when the medium length, smallest diameter #1, and medium #2 were applied. The lowest maximum displacement (Y_2 = 0.00752 mm) was observed in run 9 when the shortest length, biggest diameter #1, and biggest diameter #2 were used. The percentage of the difference between predicted and simulation for maximum stress is 1.48% and 3.56% for maximum displacement.

Table 3: CCD results for different factors combination.

Run	**Factor (coded)**			**Response (Y)**			
				Simulation		**Model Predicted**	
	A	**B**	**C**	Y_1	Y_2	Y_1	Y_2
1	0.000	-1.000	0.000	2.20181E+007	0.01978	2.25432E+007	0.02025
2	0.000	1.000	0.000	2.31022E+007	0.00919	2.25432E+007	0.00965
3	0.000	0.000	1.000	1.60108E+007	0.01162	1.58500E+007	0.01209
4	0.000	0.000	-1.000	3.55736E+007	0.01422	3.57000E+007	0.01468
5	0.000	0.000	0.000	2.30224E+007	0.01253	2.30300E+007	0.01300
6	1.000	1.000	1.000	1.64880E+007	0.00898	1.58995E+007	0.00940
7	0.000	0.000	0.000	2.30224E+007	0.01253	2.30300E+007	0.01300
8	0.000	0.000	0.000	2.30224E+007	0.01253	2.30300E+007	0.01300
9	-1.000	1.000	1.000	1.64452E+007	0.00752	1.59130E+007	0.00802
10	0.000	0.000	0.000	2.30224E+007	0.01253	2.30300E+007	0.01300
11	-1.000	-1.000	-1.000	3.52992E+007	0.01945	3.58901E+007	0.01996
12	0.000	0.000	0.000	2.30224E+007	0.01253	2.30300E+007	0.01300
13	1.000	-1.000	-1.000	3.50879E+007	0.02344	3.56225E+007	0.02386
14	0.000	0.000	0.000	2.30224E+007	0.01253	2.30300E+007	0.01300
15	1.000	0.000	0.000	2.33859E+007	0.01367	2.32336E+007	0.01432
16	1.000	-1.000	1.000	1.47369E+007	0.02088	1.54677E+007	0.02130
17	-1.000	1.000	-1.000	3.61866E+007	0.01015	3.54583E+007	0.01066
18	-1.000	0.000	0.000	2.32557E+007	0.01140	2.33742E+007	0.01168
19	-1.000	-1.000	1.000	1.47291E+007	0.01689	1.52681E+007	0.01740
20	1.000	1.000	-1.000	3.55142E+007	0.01160	3.49775E+007	0.01202

A=Length, B=Diameter #1, C=Diameter #2, Y_1=Maximum Stress, and Y_2=Maximum Displacement

3.1 Regression model and analysis of variance (ANOVA)

In this study, the most suitable fitting of regression models, maximum stress (Y_1) and maximum displacement (Y_2), were chosen based on higher-order polynomials, the significant additional terms, and the presence of aliased models through optimization software. The model responses of Y_1 and Y_2 were most suitable and fitted by a quadratic model as suggested by the software. The Model F-value of 8420.08 indicates that the model is significant, and the values of "Prob > F" are less than 0.0500. Equations (1) and (2) show the final empirical models in terms of code factors (A=length, B=diameter #1, and C=diameter #2) by considering all terms.

$$\text{Max Stress } (Y_1) = 2.303E{+}007 - 70289.50A + 5.865E{+}005B - 9.925E{+}006C + 2.739E{+}005A^2 - 4.868E{+}005\,B^2 + 2.745E{+}006C^2 - 53273.13AB + 1.168E{+}005AC + 2.692E{+}005BC \quad (1)$$

$$\text{Max Displacement } (Y_2) = 0.013 + 1.316E{-}003A - 5.300E{-}003B - 1.297E{-}003C - 9.091E{-}007A^2 + 1.949E{-}003B^2 + 3.841E{-}004C^2 - 6.337E{-}004AB + 1.250E{-}006AC - 1.625E{-}005BC \quad (2)$$

The ANOVA results from Tables 4 and 5 show the quality of the model response that was analyzed through the coefficient of determination (R-squared). The R-squared value for each empirical equation is considerably high at 0.9999 and 0.9998 for models Y_1 and Y_2, respectively. A high R-squared value implies a reliable prediction from the empirical models. The maximum stress result shows that the standard deviation value (1.163E+005) is lower than the mean value (2.430E+007). The maximum displacement shows that the standard deviation value (9.062E-005) is lower than the mean value (0.014). The pure error for both model responses is 0%, indicating that repeating results in simulation analysis are constant.

Table 4: ANOVA results of maximum stress (Y_1).

Source	Sum of Square	DF	Mean Square	F Value	Prob>F
Model	1.024E+015	9	1.138E+014	8420.08	< 0.0001
A	4.941E+010	1	4.941E+010	3.66	0.0849
B	3.440E+012	1	3.440E+012	254.51	< 0.0001
C	9.851E+014	1	9.851E+014	72885.08	< 0.0001
A2	2.062E+011	1	2.062E+011	15.26	0.0029
B2	6.516E+011	1	6.516E+011	48.21	< 0.0001
C2	2.073E+013	1	2.073E+013	1533.46	< 0.0001
AB	2.270E+010	1	2.270E+010	1.68	0.2241
AC	1.091E+011	1	1.091E+011	8.07	0.0175
BC	5.797E+011	1	5.797E+011	42.89	< 0.0001
Residual	1.352E+011	10	1.352E+010		
Lack of Fit	1.352E+011	5	2.703E+010		
Pure Error	0.000	5	0.000		

Std. Dev.	Mean	R-Squared	Adj R-Squared
1.163E+005	2.430E+007	0.9999	0.9997

Table 5: ANOVA results of maximum displacement (Y_2).

Source	Sum of Square	DF	Mean Square	F Value	Prob > F
Model	3.425E-004	9	3.805E-005	4633.97	< 0.0001
A	1.732E-005	1	1.732E-005	2109.06	< 0.0001
B	2.809E-004	1	2.809E-004	34208.03	< 0.0001
C	1.682E-005	1	1.682E-005	2048.60	< 0.0001
A^2	2.273E-012	1	2.273E-012	2.768E-004	0.9871
B^2	1.045E-005	1	1.045E-005	1272.25	< 0.0001
C^2	4.057E-007	1	4.057E-007	49.41	< 0.0001
AB	3.213E-006	1	3.213E-006	391.29	< 0.0001
AC	1.250E-011	1	1.250E-011	1.522E-003	0.9696
BC	2.113E-009	1	2.113E-009	0.26	0.6230
Residual	8.212E-008	10	8.212E-009		
Lack of Fit	8.212E-008	5	1.642E-008		
Pure Error	0.000	5	0.000		

Std. Dev.	Mean	R-Squared	Adj R-Squared
9.062E-005	0.014	0.9998	0.9995

3.2 Effect of factors on the response

The sensitivity of the independent factors was examined through a perturbation plot for length (A), diameter #1 (B), and diameter #2 (C) to the responses of maximum stress (Y_1) and maximum displacement (Y_2). Figure 2 presents the perturbation plot between factors A, B, and C to a model response Y_1 (maximum stress). The presence of each factor in the perturbation plot exhibits the influence of the independent variable on maximum stress. Factor C is the most crucial factor, and factor B slightly influences the maximum stress (Y_1). However, factor A clearly showed an almost constant plot. The increase in piston rod diameter #2 reduces the stress exerted by the load. Stress is inversely proportional to area. The increase in the piston rod area causes the stress decreases. This situation can prevent a piston rod from rupturing, leading to the bad performance of the suspension system. Furthermore, Figure 3 shows a perturbation plot of model response Y_2 (maximum piston rod displacement). The presence of factors A, B, and C in the perturbation plot indicates an influence of the independent variables to a maximum displacement. A maximum displacement is most crucially influenced by factors A and B compared with factor C. The result shows that the highest length and smallest diameter contribute to the highest maximum displacement.

Figures 4 and 5 illustrate the 3D response surface plot of the quadratic model for Y_1 and Y_2 with the two most significant factors and responses. The selection of two variables and a constant variable were selected according to the sensitivity toward the response as plotted in perturbation plots. The optimization goals are to reduce stress and displacement; thus, the minimum point was identified. Figure 4 shows the minimum stress is 1.45099E+007 N/m^2 for factor C (15 mm) and factor B (15 mm). However, the minimum displacement is 0.0084983 mm for factor B (24.8 mm) and factor A (254 mm), as shown in Figure 5. The results indicated that controlling both significant factors could yield a minimum response value.

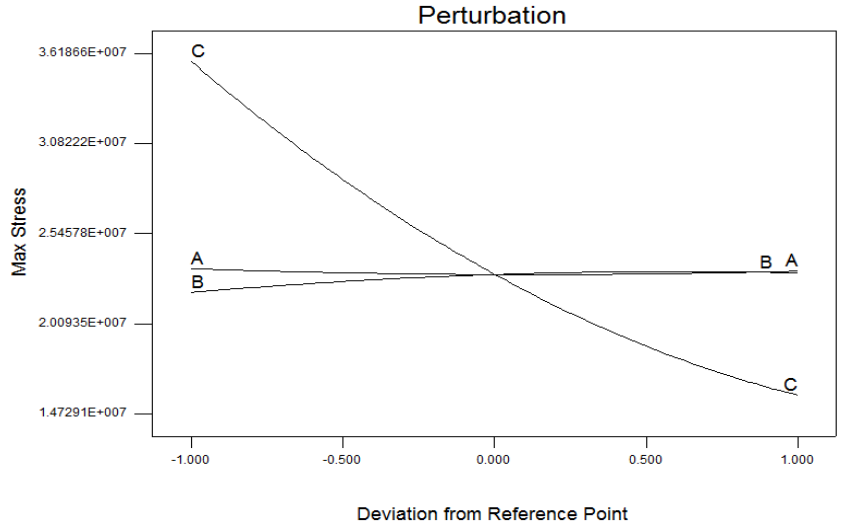

Figure 2: Perturbation plot graph of maximum stress (N/m^2).

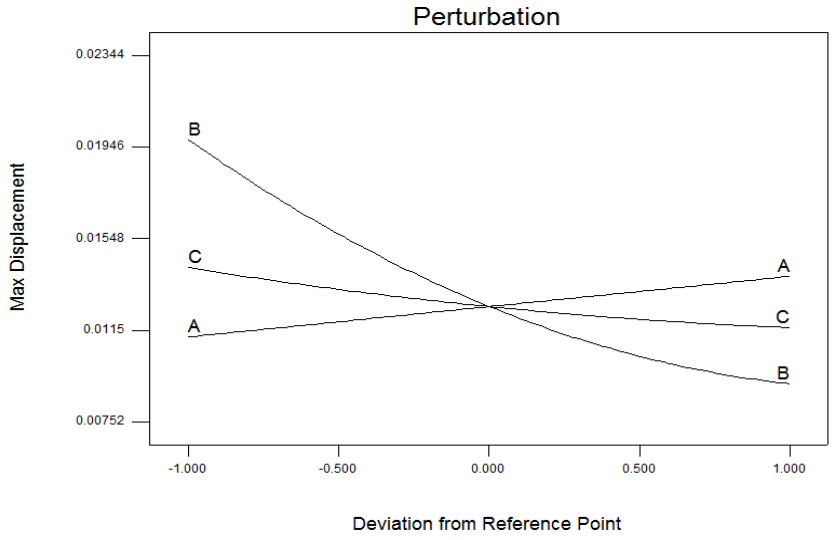

Figure 3: Perturbation plot graph of maximum displacement (mm).

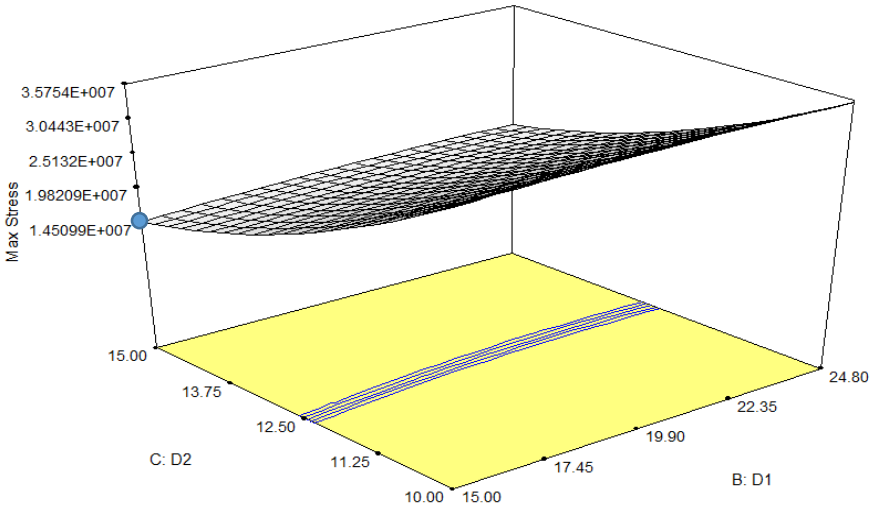

Figure 4: 3D response surface of maximum stress (Y_1).

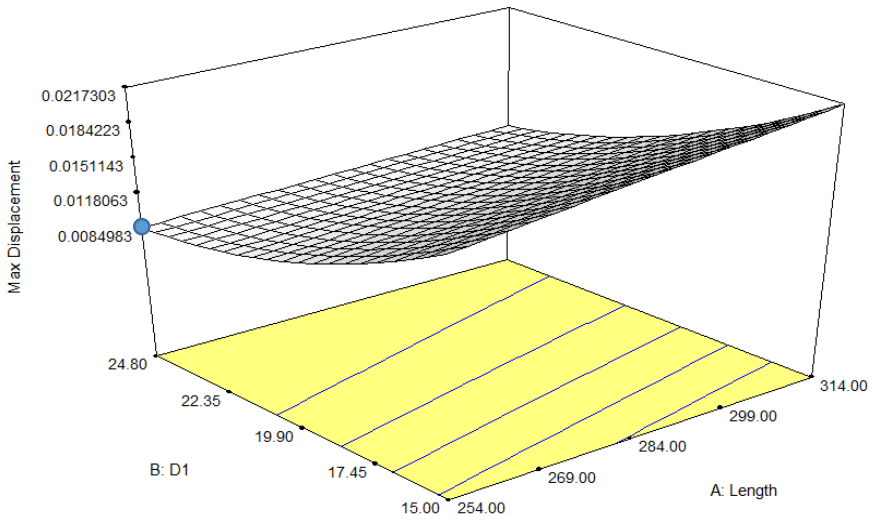

Figure 5: 3D response surface of maximum displacement (Y_2).

3.3 Optimization of design parameters

A high-reliability absorber can ensure passenger comfort in an existing suspension system. Minimum stress and displacement can improve reliability and avoid failure and rupture. The optimized absorber piston rod parameter is expected to minimize the stress and displacement in the optimization process. The optimized parameters are achieved at 254 mm in length, 24.79 mm in diameter #1, and 15 mm in diameter #2 when 2479.48 N force was applied on the piston rod. The desirability of the suggested optimized parameters is at 0.9567, almost achieving 1.00. A high desirability value indicates the best solution for the optimization study. Table 6 summarizes the optimized factors and responses value with the highest desirability.

Table 6: Optimized factors and responses.

		Optimized value
Factor	Length	254.00 mm
	Diameter #1	24.79 mm
	Diameter #2	15.00 mm
Response	Maximum stress	1.65048E+007 N/m²
	Maximum displacement	0.0075693 mm
	Desirability	0.956

3.4 Validation of simulation results

The optimized factors suggested by the optimization software are A = 254 mm, B = 24.79 mm, and C = 15.00 mm, with the minimum responses (Y_1 and Y_2). The suggested optimized factors were examined in finite element simulation to confirm the validity of the predicted model of RSM. The results were compared with the suggested model responses, as shown in Table 7. The simulation results revealed that the maximum stress (1.64452E+007 N/m²) is lower than the yield strength (6.20422E+008 N/m²). This situation indicates that the piston rod will not fail and rupture easily. The maximum stress occurs between diameters #1 and #2, located at the piston rod's bottom. In contrast, maximum displacement occurs at the top of the piston rod. Besides, the percentage difference between the response model and simulation is low for both stress (0.36%) and displacement (0.6%). Therefore, each factor's optimum values were successfully determined using RSM.

Table 7: The validation of model response and simulation for optimized factors.

	Response (Y)	
	Y_1 - Stress	Y_2 - Displacement
Model Response	1.65048E+007	0.007569
Simulation	1.64452E+007	0.007524
% Difference	0.36%	0.6%

4. CONCLUSION

The RSM optimization was successfully conducted for a car absorber piston rod design parameter via finite element analysis. Twenty simulation runs were performed at different levels of parameters in order to get optimum results. The highest maximum stress (Y_1), which is 3.55736E+007 N/m^2, was observed in run 4, while the lowest maximum stress (Y_1), which is 1.47291E+007 N/m^2, was observed in run 19. Hence, a higher maximum displacement (Y_2) which is 0.01978 mm, was observed in run 1, while the lowest maximum stress (Y_2), which is 0.00752 mm, was observed in run 9. Factors B and C were the most significant factor that affected stress. However, displacement was crucially influenced by factors A and B. The RSM results revealed that the optimum values were A = 254 mm, B = 24.79 mm, and C = 15.00 mm. The maximum stress and displacement were reduced to 1.65048E+007 N/m^2 and 0.0075693 mm when using these parameter values with the desirability of 0.956.

ACKNOWLEDGEMENTS
The author gratefully thanks the Faculty of Mechanical Engineering & Technology, Universiti Malaysia Perlis (UniMAP), for the facilities support. The author would like to thank the supervisor for his guidance and support throughout this project.

REFERENCES

[1] Ahmed, M. R., Yusoff, A. R., & Romlay, F. R. M. Adjustable valve semi-active suspension system for passenger car. International Journal of Automotive and Mechanical Engineering, vol 16, issue 2 (2019) pp.6470-6481.
[2] Aboazoum, A. An Overview of the most Common Vehicle Suspension Problems. Brilliance: Research of Artificial Intelligence, vol 2, issue 3 (2022) pp.120-124.
[3] Gatti, G. Optimizing elastic potential energy via geometric nonlinear stiffness. Communications in Nonlinear Science and Numerical Simulation, vol 103, (2021) pp.106035.
[4] Ikechukwu, O., Aniekan, I., Ebunilo, P. O., & Ikpe, E. Investigation of a vehicle tie rod failure in relation to the forces acting on the suspension system. American Journal of Engineering Research, vol 5, issue 5 (2016) pp.208-217.
[5] Soliman, A. M. A., & Kaldas, M. M. S. Semi-active suspension systems from research to mass-market–A review. Journal of Low Frequency Noise, Vibration and Active Control, vol 40, issue 2 (2021) pp.1005-1023.
[6] Łuczko, J., & Ferdek, U. Non-linear analysis of a quarter-car model with stroke-dependent twin-tube shock absorber. Mechanical Systems and Signal Processing, vol 115, (2019) pp.450-468.
[7] Farfan-Cabrera, L. I. Tribology of electric vehicles: A review of critical components, current state and future improvement trends. Tribology International, vol 138, (2019) pp.473-486.
[8] Prasad, G. Engine Retarders. In Design and Development of Heavy Duty Diesel Engines Springer, Singapore. (2020) pp. 637-678.

[9] Liu, Y., Zhang, J., & Cheng, X. Experimental and dynamic study of the piston rod lateral friction for the twin-tube hydraulic shock absorber. Shock and Vibration, vol 10, issue 3 (2003) pp.169-177.
[10] Lu, Z., Wang, Z., Zhou, Y., & Lu, X. Nonlinear dissipative devices in structural vibration control: A review. Journal of Sound and Vibration, vol 423, (2018) pp.18-49.
[11] Cebon, D. Vehicle-generated road damage: a review. Vehicle system dynamics, vol 18, issue 1-3 (1989) pp.107-150.
[12] Leong, W. C., Abdullah, M. Z., & Khor, C. Y. Optimization of flexible printed circuit board electronics in the flow environment using response surface methodology. Microelectronics Reliability, vol 53, issue 12 (2013) pp.1996-2004.
[13] Veljković, V. B., Veličković, A. V., Avramović, J. M., & Stamenković, O. S. Modeling of biodiesel production: Performance comparison of Box–Behnken, face central composite and full factorial design. Chinese Journal of Chemical Engineering, vol 27, issue 7 (2019) pp.1690-1698.
[14] Lau, C. S., Abdullah, M. Z., & Khor, C. Y. Optimization of the reflow soldering process with multiple quality characteristics in ball grid array packaging by using the grey-based Taguchi method. Microelectronics International, vol 30, issue 3 (2013) pp.151-168.
[15] Ma, Z., Wang, H., Hui, B., Jelagin, D., You, Z., & Feng, P. Optimal design of fresh sand fog seal mortar using response surface methodology (RSM): Towards to its workability and rheological properties. Construction and Building Materials, vol 340, (2022) pp.127638.
[16] Hirkude, J. B., & Padalkar, A. S. Performance optimization of CI engine fuelled with waste fried oil methyl ester-diesel blend using response surface methodology. Fuel, vol 119, (2014) pp.266-273.
[17] Faizal, W. M., Ghazali, N. N. N., Khor, C. Y., Badruddin, I. A., Zainon, M. Z., Yazid, A. A. & Razi, R. M. Computational fluid dynamics modelling of human upper airway: A review. Computer methods and programs in biomedicine, vol 196, (2020) pp.105627.
[18] Aziz, M. S. A., Abdullah, M. Z., & Khor, C. Y. Influence of PTH offset angle in wave soldering with thermal-coupling method. Soldering & Surface Mount Technology, vol 26, issue 3 (2014) pp.97-109.
[19] Sadjadi, E. N., Garcia, J., Molina Lopez, J. M., Borzabadi, A. H., & Abchouyeh, M. A. Fuzzy model identification and self learning with smooth compositions. International Journal of Fuzzy Systems, vol 21, issue 8 (2019) pp.2679-2693.
[20] Aziz, M. A., Abdullah, M. Z., Khor, C. Y., & Azid, I. A. Optimization of pin through hole connector in thermal fluid–structure interaction analysis of wave soldering process using response surface methodology. Simulation Modelling Practice and Theory, vol 57, (2015) pp.45-57.